tum, $L = Mvr$, we assume that the "radius" appropriate for the interacting nucleons in the inverse of the pion mass. Thus,

$$L^2 = \left(\frac{Mv}{M_\pi}\right)^2 = \frac{2ME}{M_\pi{}^2} \approx \frac{E\ (\text{in MeV})}{10\ \text{MeV}} .$$

*Work supported in part by the U. S. Atomic Energy Commission under Contract No. ORO 3765-27.

†Present address: Department of Physics, Kansas State University, Manhattan, Kansas 66502.

[1]M. K. Banerjee, C. A. Levinson, M. D. Shuster, and D. A. Zollman, University of Maryland Technical Report No. 70-081 (unpublished).

[2]S. Fubini and G. Furlan, Ann. Phys. (N.Y.) 48, 322 (1968).

[3]S. Adler, Phys. Rev. 139, B1638 (1965).

[4]D. Beder, Nuovo Cimento 56A, 625 (1968); 58A, 908(E) (1968).

[5]M. Schillaci, R. Silbar, and J. Young, Phys. Rev. Letters 21, 711, 1030(E) (1968); Phys. Rev. 179, 1539 (1969).

[6]A short review of pion production in nucleon-nucleon collisions appears in D. Koltun, in *Advances in Nuclear Physics*, edited by M. Baranger and E. Vogt (Plenum Press, New York, 1969), Vol. 3, pp. 160–167.

[7]D. Koltun and A. Reitan, Phys. Rev. 141, 1413 (1966); A. Reitan, Nucl. Phys. B11, 170 (1969).

[8]See, for example, S. Weinberg, Phys. Rev. Letters 17, 168 (1966).

[9]M. Schillaci and R. Silbar, to be published.

[10]D. Cochran, P. Dean, P. Gram, E. Knapp, E. Marin, D. Nagle, R. Perkins, W. Schlaer, E. Theriot, and H. Thiessen, to be published (quoted in Ref. 19).

[11]R. Reid, Jr., Ann. Phys. (N.Y.) 50, 411 (1968).

[12]T. Hamada and I. Johnston, Nucl. Phys. 34, 382 (1962).

[13]C. Bressel, A. Kerman, and B. Rouben, Nucl. Phys. A124, 624 (1969).

[14]E. Redish, G. Stephenson, Jr., and G. Lerner, private communication.

[15]This approximation originally appeared in K. Watson, Phys. Rev. 88, 1163 (1952).

PHYSICAL REVIEW C VOLUME 2, NUMBER 6 DECEMBER 1970

Elastic Scattering of 36.0- and 46.3-MeV Neutrons from Deuterium*

Juan L. Romero,† J. A. Jungerman, F. P. Brady, W. J. Knox, and Y. Ishizaki‡
Crocker Nuclear Laboratory and Physics Department, University of California, Davis, California 95616
(Received 5 August 1970)

The differential cross sections for elastic scattering of 36.0- and 46.3-MeV neutrons from deuterium were measured over an angular range of 15 to 170° c.m. The cross section agrees well in shape and absolute value with that for p-d scattering. A slightly more pronounced minimum seems to be present in the n-d results. From measured values of the total n-d cross sections, we obtain the values 154 ± 6 and 116 ± 5 mb at 36.0 and 46.3 MeV, respectively, for the n-d nonelastic cross section.

I. INTRODUCTION

The interaction of two neutrons and one proton is the simplest and the most fundamental three-body problem in nuclear physics. The lack of any Coulomb interaction among the particles simplifies the theoretical description of the system. The three-body problem was set on a sound mathematical basis by the work of Faddeev.[1] Independently, the introduction in 1962 of an S-wave separable potential in the Schrödinger equation by Mitra[2] and also by Amado[3] permitted an exact treatment of the dynamical aspects of the three-nucleon problem. This approach has been very successful in predicting low-energy properties of the three-nucleon system[4–6]; in particular, n-d differential cross sections up to 14 MeV. Inclusion of higher partial waves and tensor forces seems necessary to describe polarization and medium-energy, 20–60-MeV, n-d elastic scattering. Work in this direction is currently being attempted by several groups.[7,8]

Mainly because of the lack of intense neutron beams, no neutron n-d elastic scattering has as yet been published in the medium-energy region although incomplete work has been reported between 18.6 and 20.5 MeV at Los Alamos[9] and at 28 MeV at Lyon.[10] The present work involves measurements of n-d elastic scattering at 36.0 and 46.3 MeV. Preliminary results of some of this work have been reported.[11] Energies were selected to be close to those of the p-d measurements performed at the University of California, Los Angeles (UCLA) in order to have a more direct

comparison between the two systems of three nucleons. To normalize the n-d data, measurements were also done on the n-p elastic scattering cross sections at the above indicated energies. These data supplemented the more extensive measurements made at Harwell.[12]

II. EXPERIMENTAL TECHNIQUES

The experiment was performed using the 76-in. cyclotron of the Crocker Nuclear Laboratory, Davis. A description of the neutron beam line is given elsewhere.[13] Neutron production studies at Davis[14] as well as the work done at Rutherford High Energy Laboratory[15] indicate that ^{7}Li is the most practical target for producing a monochromatic, high-yield beam using a (p, n) reaction. The high-energy peak of the neutron beam was selected in each case by using a time signal from a beam-pickoff unit placed just in advance of the neutron-producing target. Figure 1 shows a neutron spectrum from a ^{7}Li target as used in this experiment. Typically, a 7-μA proton beam was incident on a target whose thickness corresponded to a loss of about 2 MeV. This beam gives a flux of 5.2×10^5 neutrons/sec on a 1.8-cm^2 area at the scintillating target position with an energy spread of about 2.0 MeV full width at half maximum.

For neutron scattering angles greater than 90°, the neutron beam was scattered by a $(CD_2)_n$ or $(CH_2)_n$ target and the recoil charged particle detected in a ΔE-E telescope. The ΔE-E signals were used to identify the recoil particles. Energy spectra were recorded separately for protons and deuterons by storing the identification pulse versus the energy pulse in a two-dimensional analyzer. For forward neutron angles the neutron beam was scattered into a neutron detector by a liquid scintillator containing ordinary heptane or deuterated heptane. A two-parameter analyzer recorded the recoil charged-particle energy in the liquid scintillator versus the time of flight of the neutron between the scintillating target and the neutron detector.

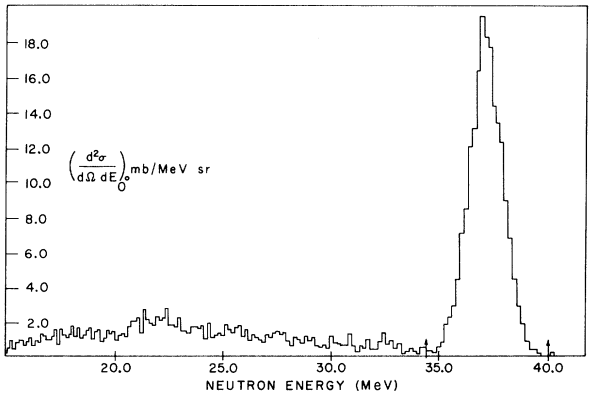

FIG. 1. Neutron spectrum from bombardment of a 0.128-in. ^{7}Li target with 39.3-MeV protons.

A. Beam Energy

A convenient feature of the unpolarized neutron beam facility at Davis is the possibility of having the proton beam available at the exit of the collimator. This permits the energy of the incident proton beam to be determined using a cross-over technique.[16,17] In this method one observes the relative positions of the peaks for two different reactions as a function of the angle of the detector. In this experiment the two reactions, ^{2}H$(p, d)^1$H and ^{12}C$(p, d)^{11}$B ($Q=-16.50$ MeV), were used to measure the beam energy. These reactions were observed using a small proton beam (a few nA) incident on a deuterated polyethylene target. The emitted deuterons were detected using a ΔE-E telescope and a particle identifier. The cross-over angle for these reactions is more sensitive to beam energy than that for protons elastically scattered from hydrogen and inelastically scattered by carbon-12. Moreover, the deuteron spectra are clean and unambiguous. In the region between 30–45 MeV, the cross-over angle changes roughly 0.1° for a 0.1-MeV change in the incident beam energy. The neutron beam energy was obtained to ±200 keV for each experimental run.

B. Solid-State-Detector Technique

For detection of deuteron recoils corresponding to large neutron c.m. scattering angles, a telescope of solid-state ΔE-E detectors was used. In order to get a good timing signal the ΔE detector has to be rather thin, of the order of 200 μ. A fast preamplifier in conjunction with a 260 ORTEC time-pickoff unit was used which was sensitive down to about 200-keV electron energy. The ΔE and E detectors each had an area of 300 mm^2. The ΔE detector was a 200-μ fully depleted surface-barrier detector and the E detector was lithium-drifted and 5 mm in depth. A veto counter consisting of an NE102 plastic scintillator 76×76 mm and 250 μ thick was employed ahead of the deuterated polyethylene target to eliminate charged-particle contributions to the scattering.

Figure 2 shows a block diagram of the electronics for this system. The linear pulses from the E and ΔE detector previously amplified are linear-gated by a coincidence requirement C. If the gate is open, they are passed to the particle identifier. This provides an E plus ΔE and a particle-identification pulse. These two pulses are taken to a 64×64 two-parameter multichannel analyzer. The

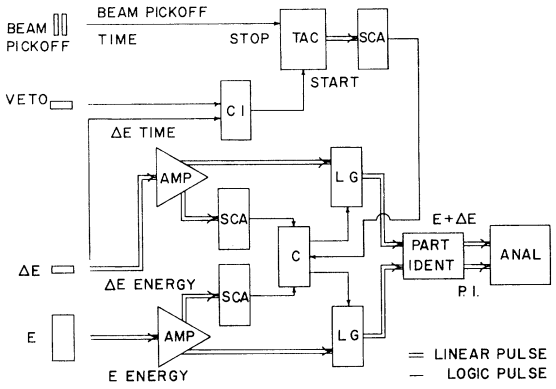

FIG. 2. Block diagram for solid-state-detector technique. TAC = time-to-amplitude converter. SCA = single-channel analyzer. LG = linear gate. C = coincidence. AMP = amplifier. CI = anticoincidence. ANAL = multichannel analyzer.

coincidence requirement C involves a slow coincidence between the ΔE pulse and E pulse and a fast-time pulse. A time-of-flight spectrum is obtained from the time-to-amplitude converter (TAC) with the fast ΔE timing pulse and the beam-pickoff timing pulse as the start and stop. This TAC spectrum is used to define the incident neutron beam. A single-channel analyzer selects the TAC peak of the neutron spectrum as depicted in Fig. 1.

As an over-all check of the electronics, a small proton beam was directed onto a deuterated polyethylene target. Elastic protons scattering from carbon and deuterium as well as recoiling deuterium nuclei provided calibration of the system. We compared the elastic protons scattered from deuterium with the elastic protons scattered from carbon in a deuterated polyethylene target. This procedure was repeated with an ordinary polyethylene target, this time integrating elastic protons from hydrogen as well as from carbon. In this way we were able to obtain the ratios of the p-d and p-p cross sections at two different angles. Table I shows the results of using 48.1-MeV protons. The excellent agreement with published data on the cross sections indicates that the particle-identification system is better than 98% efficient and that the time-pickoff system is also good to the same accuracy.

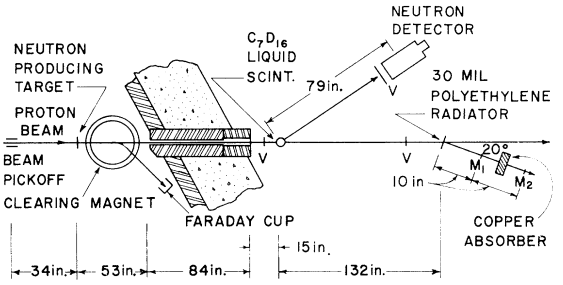

FIG. 3. Experimental setup using a C_7D_{16} liquid scintillator target and a neutron detector.

C. Scintillating-Target-Neutron-Detector Technique

For measurement of neutrons scattered at c.m. angles less than 90° a scintillating target was used. Figure 3 shows the geometry. The neutron was detected in coincidence with the deuteron recoil in the scintillating target. Two-parameter analysis was made of the recoiling deuteron energy and the time of flight of the neutron. Since the scintillating target is placed in the incident beam, the detector has a high counting rate, around 100 kHz. The linear analysis of the deuteron energy is then very questionable unless a reasonable counting rate is presented to the slow linear amplifier. This was achieved in the present experiment by

TABLE I. Comparison of the ratios $\sigma_{p-d}^{\text{c.m.}}(\theta)/\sigma_{p-p}^{\text{c.m.}}(\theta)$ and $\sigma_{p-c}^{\text{c.m.}}(\theta)/\sigma_{p-p}^{\text{c.m.}}(\theta)$ for 48.1-MeV protons at two angles. We assume $\sigma_{pp}^{\text{c.m.}}(72°) = \sigma_{pp}^{\text{c.m.}}(80°) = 8.82 \pm 2\%$ (mb/sr).

Particle angle (deg)	Target	Detected particle	$\theta_{p-d}^{\text{c.m.}}$ (deg)	$\sigma_{p-d}^{\text{c.m.}}/\sigma_{p-p}^{\text{c.m.}}$ This work	$\sigma_{p-d}^{\text{c.m.}}/\sigma_{p-p}^{\text{c.m.}}$ Published[a,b]	$\theta_{p-c}^{\text{c.m.}}$ (deg)	$\sigma_{p-c}^{\text{c.m.}}/\sigma_{p-p}^{\text{c.m.}}$ This work	$\sigma_{p-c}^{\text{c.m.}}/\sigma_{p-p}^{\text{c.m.}}$ Published[c]
36	$(CD_2)_n$	proton	53.4	$1.13 \pm 4\%$	$1.19 \pm 2\%$	39.0	$2.85 \pm 5\%$	$2.85 \pm 2\%$
	$(CH_2)_n$	proton						
40	$(CD_2)_n$	proton	59.1	$1.10 \pm 4\%$	$1.02 \pm 2\%$	43.2	$2.11 \pm 5\%$	$2.04 \pm 2\%$
	$(CH_2)_n$	proton						
40	$(CD_2)_n$	deuteron	99.3	$0.28 \pm 5\%$	$0.28 \pm 2\%$			
	$(CH_2)_n$	proton						

[a] See Ref. 29.

[b] R. Wilson, *The Nucleon-Nucleon Interaction, Experimental and Phenomenological Aspects* (Interscience Publishers, Inc., New York, 1963).

[c] J. A. Fannon *et al.*, Nucl. Phys. A97, 263 (1967).

sending the energy pulse into a fast linear gate which opened with a requirement of coincidence between the neutron detector and the scintillating target. This reduced the counting rate in the linear system to less than 200 counts/sec.

The neutron detector was a cylinder of NE102 plastic scintillator 127 mm in diameter by 0.304 m in length sealed directly to the face of a 127-mm XP1040 photomultiplier. An ORTEC 268 fast-cross-over base was used to eliminate walk. The efficiency of the detector as a function of the neutron energy has been measured in a separate experiment.[18-20] The liquid scintillator targets were ordinary heptane or deuterated heptane or a known mixture of them as supplied by Nuclear Enterprises, Inc. Each cylindrical scintillator came encapsulated in a 1-mm Pyrex cell which was 38.1 mm long and either 31.9 or 19.1 mm in diameter. The scintillators were coupled to an RCA 8575 photomultiplier by a cone-shaped Lucite light guide. Figure 4 shows a block diagram of the electronics for the liquid scintillator set-up.

D. Monitors

Two monitors were used and intercompared during every run. One of them consisted of the integration of the incident proton beam by a Faraday cup after the beam was deflected by the clearing magnet. In the second monitor, the incident neutron beam at 0° was detected with a counter telescope. This monitor is indicated in Fig. 3. The counters were set at 20° to the beam line and used a 0.76-mm polyethylene converter. Time of flight selected only the peak of the neutron spectrum, and a copper absorber between the two counters eliminated neutrons from previous bursts.

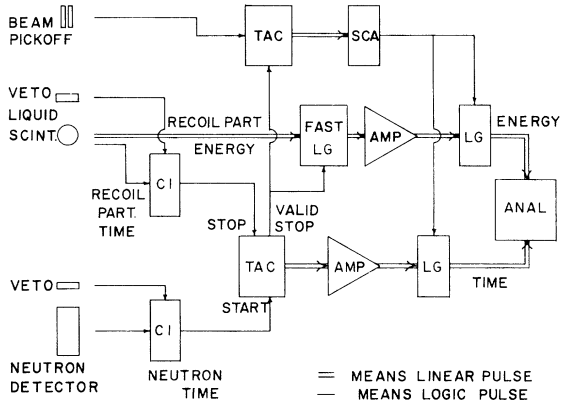

FIG. 4. Block diagram for liquid-scintillator-neutron-detector technique. Notation as in Fig. 2.

III. MEASUREMENTS AND ANALYSIS

A. Solid-State-Detector Measurements

Timing of the veto detector was set by placing it in front of the ΔE detector and displaying signals in a triggered scope. The same technique was used to set the timing of the monitor telescope. At a beam intensity of 7 μA, an average of two hours running time was used for the deuterated polyethylene target and one hour for the ordinary polyethylene target for each angle measured. A thin carbon target gave the background due to carbon in the targets.

Figure 5 shows several slices of the deuteron spectra taken with 46.3-MeV neutrons at a lab recoil angle of 15°. The prominent peak in (a) and (b), also present in (c), corresponds to the pickup reaction on carbon, $^{12}C(n,d)^{11}B$ ($Q=-13.7$ MeV).

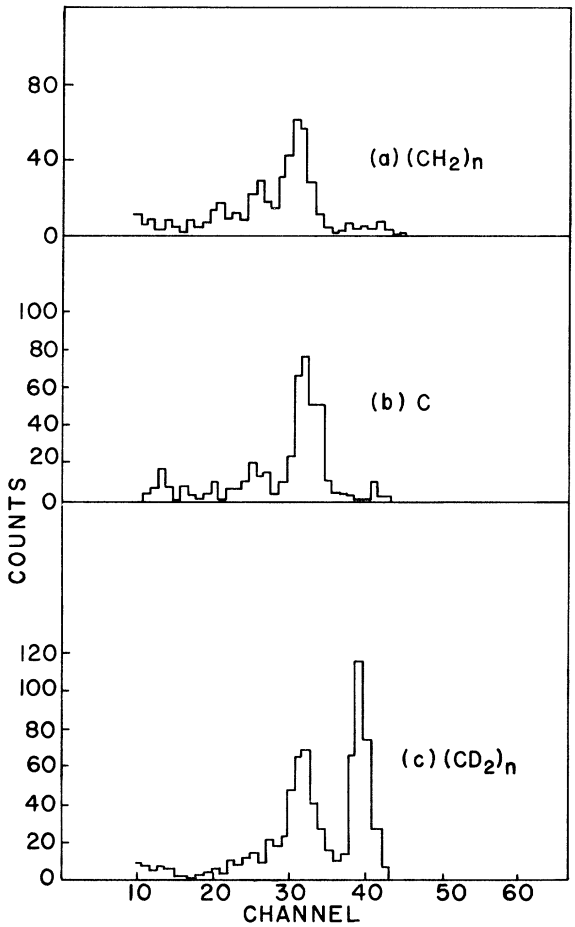

FIG. 5. Deuteron spectra at 15° produced by bombardment of polyethylene, carbon, and deuterated polyethylene with 46.3-MeV neutrons. All spectra are normalized to the same number of carbon atoms and the same number of counts in the monitor. The peak at channel 32 is due to the reaction $^{12}C(n,d)^{11}B$ ($Q=-13.7$ MeV).

The peak at channel 40 in (c) is due to recoil deuterons of 34.4 MeV from deuterium.

Every run was recorded on magnetic tape and a 64×64 matrix printout was obtained. The zone of the peaks was also plotted in a high-speed data reducing program, GLORY.[21] The integration was straightforward with the carbon subtraction being made directly. The background under the deuteron peak was on the average around 10% increasing up to 50% at the minimum of the differential cross section. In the case of the ordinary polyethylene target, the background was less than 10%.

Corrections were applied to the data due to neutron attenuation in air and the nuclear interaction of protons and deuterons in the detectors. For 40-MeV protons and deuterons this latter effect is around 2.8% for silicon, decreasing nearly to 0 at 10 MeV.

B. Scintillating-Target-Neutron-Detector Measurements

Before every run the electronics were set and tested using a 1-mCi ^{22}Na source to provide 180° γ coincidences between the liquid scintillator and the neutron detector. A ^{207}Bi source was used to set the timing for the monitor. The neutron-detector threshold was set using a ^{60}Co source following the method used when the neutron detector was calibrated.[19] A 1-MeV electron threshold was used. The setting of the threshold was checked during and at the end of the experiment. For the forward angles it was necessary to increase the scintillating-target high voltage in order to detect the small-energy recoil particles. Typical runs lasted about 30 min for a 4-μA beam. Every run was recorded on magnetic tape and a number of scalers were used to monitor the different detectors. A 64×64 matrix printout around the peaks was obtained directly from the magnetic tape. Every peak was integrated by making cuts along the time axis and then integrating the peaks in the individual energy spectra. A so-called energy background was assigned to each of these peaks by averaging the counts in the energy spectrum on both sides of the peak. A second background estimate, called the time background, was obtained by summing the counts at the same energy channels with a time region outside the peak. The actual background of the peak was assumed to be the average of the separately determined time and energy backgrounds.

The following corrections were considered and applied to the data.

1. Beam Attenuation

Corrections were applied for the attenuation of the incident neutrons in Pyrex, the scintillator itself, and air. Attenuation of the incident beam at the center of the target was around 10%. Attenuation of the scattered neutrons ranged from 10 to 20%.

2. Edge Effect

The edge effect corresponds to the case when a valid event is lost because the recoil particle enters the wall of the scintillator before losing enough energy to be detected. A calculation was performed to determine this effect. First the minimum range in the scintillator is found in which the recoil particle deposits enough particle energy to be in the peak, and then the fraction of the target corresponding to these recoils was obtained. The effect is larger for smaller scintillators and for large energies of the recoil particle. Since it is proportional to the range of the particle, it is

TABLE II. Some typical counting rates and corrections. Incident neutron energy = 36.0 MeV. Incident neutron beam attenuation is 10% for the 31.9-mm-diam liquid scintillator and 6.8% for 19.1-mm-diam.

Reaction	Scintillator target	Diameter (mm)	Angle (deg)	Peak (counts)	BKG (counts)	Neutron energy (MeV)	Neutron efficiency (%)	Scattered neutron attenuation (%)	Recoil energy (MeV)	Edge effect (%)
^{1}H(n,n)^{1}H	C_7H_{16}	31.9	10	3560	384	35.0	44.0	11.0	1.1	<0.5
		31.9	30	3283	214	26.9	44.0	13.0	9.1	<0.5
		19.1	30	3165	464	26.9	44.0	9.3	9.1	6.0
		31.9	50	1988	201	14.7	37.0	17.0	21.3	8.0
		19.1	50	2147	469	14.7	37.0	11.9	21.3	14
^{2}H(n,n)^{2}H	C_7D_{16}	31.9	10	3120	210	35.5	44.0	12.5	0.6	<0.5
		31.9	30	1568	143	31.4	44.0	13.3	4.7	<0.5
		19.1	30	3869	546	31.4	44.0	8.6	4.7	<0.5
		31.9	50	1961	479	24.6	43.4	15.4	11.3	1.3
		19.1	50	1692	428	24.6	43.4	9.8	11.3	2.3
		31.9	60	1208	380	21.1	42.3	17.2	15.0	3.7
		19.1	60	877	238	21.0	42.3	10.9	15.0	6.5

TABLE III. Some typical counting rates and corrections. Incident neutron energy = 46.3 MeV. Incident neutron beam attenuation is 7.9% for 31.9-mm-diam liquid scintillator and 6.3% for 19.1 mm diam.

Reaction	Scintillator target	Diameter (mm)	Angle (deg)	Peak (counts)	BKG (counts)	Neutron energy (MeV)	Neutron efficiency (%)	Scattered neutron attenuation (%)	Recoil energy (MeV)	Edge effect (%)
$^1H(n,n)^1H$	C_7H_{16}	31.9	10	4250	1295	44.9	43.8	8.7	1.4	<0.5
		31.9	30	5594	876	34.6	44.0	10.5	11.8	2.4
		19.1	30	2950	567	34.6	44.0	7.6	11.8	4.2
		31.9	50	2774	653	18.9	40.9	13.7	27.5	17.6
		19.1	50	1337	486	18.9	40.8	10.7	27.5	30.8
$^2H(n,n)^2H$	C_7D_{16}	31.9	10	3063	547	45.6	43.8	9.9	0.7	<0.5
		31.9	30	3179	702	40.3	43.6	10.7	6.0	<0.5
		19.1	30	3392	773	40.3	43.6	10.7	6.9	<0.5
		31.9	50	2412	1063	31.7	44.0	12.5	14.7	2.4
		19.1	50	1582	760	31.7	44.0	7.9	14.7	4.2
		31.9	60	3221	2002	27.0	43.7	13.8	19.3	5.4

larger for protons than for deuterons. The maximum edge effect in our final n-p data was 15%, while for most of the data it was less than a 1% correction.

3. Multiple Scattering of Neutrons

The multiple-scattering losses are roughly proportional to the size of the scintillator. While these corrections are significant for low-energy neutrons[22,23] they diminish with increasing neutron energies. Several comparisons at different angles were done between 31.9-mm-diam and 19.1-mm-diam scintillators in order to measure this effect. These comparisons covered most of the angular region. The data taken with both scintillators were consistent within 6% with no systematic deviations. We concluded that this effect was at most on the order of 6%, since the extrapolation to 0 thickness of the scintillating target is reasonably accomplished with a measurement at 31.9 and 19.1 mm diam. The data taken with the smaller scintillator were included and averaged with those from the large ones.

4. Possible Impurities Under Elastic Peaks

Reactions such as $D(n,n')n,p$, $C(n,n)C$, $C(n,n')$-3^4He ($Q=-7.26$ MeV), and $C(n,n')C+\gamma$ were considered to be well discriminated against with the present technique. Mechanisms such as $C(n,n)C$ and $C(n,n')3^4He$ have very small light output in the liquid scintillators compared with protons and deuterons.[24] Tables II and III give some typical counting rates, background, efficiency of the neutron detector, and corrections for neutron attenuation and edge effects for 36- and 46-MeV neutrons.

C. Normalization Procedure

The angular distributions from both techniques, i.e., solid-state-detector and scintillating-target techniques, were normalized in the angular overlap region. This was done since the actual data for the two methods were taken in different runs and one could expect systematic variations in the monitors. The normalization factor was obtained through the overlap region between both techniques by averaging the ratios with the same c.m. angle. This procedure gave the angular distribution at 36 and 46.3 MeV for both n-p and n-d scattering. An independent n-d to n-p normalization was obtained at some angles for a mixed scintillator target containing 58% C_7D_{16} and 42% C_7H_{16}. This ratio was found to be consistent with that obtained by using unmixed targets.

The absolute differential cross sections were obtained at each energy by integrating the n-p angular distribution to obtain the corresponding total n-p cross section. The angular distribution was integrated by first fitting it to a Legendre-polynomial expansion using a least-squares-fitting program HESSIT.[25] If the constant of this expansion is a_0, the total cross section is $\sigma_{\text{total}} = 4\pi a_0$. The comparison of $4\pi a_0$ to the experimental total n-p cross section gives the normalization factor. For each energy this factor was applied to both the n-p and n-d angular distributions.

Although the error in the determination of a_0 by the fitting procedure is less than 2%, because of the scatter of individual points in the n-p angular distribution, the over-all normalization error is

TABLE IV. n-p total cross section.

Energy (MeV)	σ_{np} (mb)
36.0	248.4 ± 2.5
46.3	184.1 ± 1.8

estimated to be ±10%.

In the normalization procedure already described, the total n-p cross sections at 36.0 and 46.3 MeV are required. These cross sections together with the n-d and other total cross sections were measured in a separate experiment.[26-28] Table IV shows the results obtained for the n-p total cross sections at 36.0 and 46.3 MeV.

IV. RESULTS AND DISCUSSION

Figures 6 and 7 show the n-d differential cross section at 36.0 and 46.3 MeV, respectively, and also the p-d differential cross section at 35.0 and 46.3 MeV as measured at UCLA.[29] There is general over-all agreement both in shape and absolute values between the n-d and p-d results. The absence of the Coulomb interference in the forward direction is clearly observed in the n-d cross section. The experimental n-d angular acceptance is about 10° in the center of mass so that unfolding of our data at 36.0 MeV would lower the minimum by an additional 8%. A similar unfolding should be negligible for the p-d data. Table V gives the differential cross sections at 36.0 MeV, and Table VI gives the corresponding cross sections at 46.3 MeV.

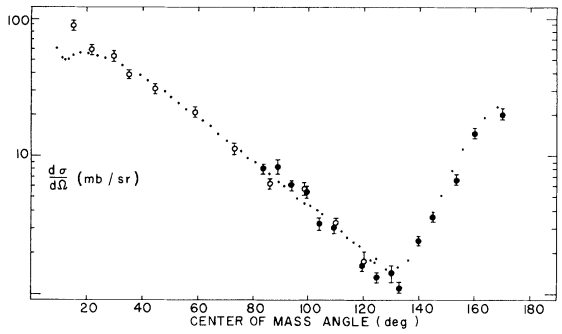

FIG. 6. Differential cross section for n-d scattering at 36.0 MeV. Open circles correspond to data taken with the liquid-scintillator-neutron-detector techniques. Black circles are data taken with the solid-state-detector technique. The dots indicate UCLA measurements for p-d at 35.0 MeV.

The errors quoted include those due to statistics, background subtraction, errors in the efficiency of the neutron detector, in target thickness, and in the corrections for attenuation, multiple scattering, and edge effects.

The neutron spectrum used for each measurement was monitored continuously by observing the time-of-flight spectrum. Because of the modest

TABLE V. Differential cross section for n-d elastic scattering at 36.0 MeV.

Lab angle (deg)	Particle detected	c.m. angle (deg)	$(d\sigma/d\Omega)$c.m. (mb/sr)	Error (mb/sr)
10	n	15.1	95.7	7.7
15	n	22.6	62.0	5.0
20	n	30.1	56.0	4.2
25	n	37.5	40.8	3.3
30	n	44.8	32.1	2.5
40	n	59.2	21.5	1.7
50	n	73.0	11.6	0.9
47.5	d	84.2	8.1	0.7
60	n	86.2	6.3	0.5
45	d	89.2	8.4	1.0
42.5	d	94.3	6.1	0.5
40	d	99.3	5.5	0.5
70	n	98.6	5.8	0.6
37.5	d	104.4	3.2	0.3
80	n	110.0	3.2	0.2
35	d	109.5	3.1	0.3
90	n	120.5	1.7	0.3
30	d	119.5	1.6	0.1
27.5	d	124.5	1.3	0.1
25	d	129.6	1.4	0.2
23.5	d	132.6	1.1	0.1
20	d	139.7	2.4	0.2
17.5	d	144.7	3.6	0.3
15	d	149.8	7.6	0.6
13.5	d	152.8	6.7	0.4
10	d	159.8	14.8	0.9
5	d	169.9	20.1	1.7

TABLE VI. Differential cross section for n-d elastic scattering at 46.3 MeV.

Lab angle (deg)	Particle detected	c.m. angle (deg)	$(d\sigma/d\Omega)$ c.m. (mb/sr)	Error (mb/sr)
10	n	15.2	70.7	5.8
15	n	27.7	52.2	4.2
20	n	30.2	41.9	3.5
25	n	37.6	32.0	2.8
30	n	44.9	23.4	1.8
35	n	52.2	15.4	1.3
40	n	59.3	14.5	1.1
45	n	66.3	9.3	0.9
55	d	69.7	9.8	0.8
50	n	73.1	6.4	0.5
50	d	79.7	7.4	0.5
55	n	79.8	5.0	0.5
60	n	86.3	3.8	0.4
45	d	89.7	3.6	0.2
70	n	98.7	2.3	0.3
40	d	99.7	2.6	0.2
35	d	109.7	1.9	0.2
30	d	119.7	1.4	0.2
25	d	129.8	0.88	0.16
20	d	139.8	1.5	0.2
15	d	149.8	3.0	0.2
10	d	159.9	6.6	0.4
5	d	170.0	11.9	0.8

variation of the n-d differential cross section with energy, the error in its measurement is negligible due to small changes in the neutron energy spectrum.

The errors given are the relative errors for individual points in the angular distribution. Not included is the normalization error of ±10% described above which is systematic, i.e., is the same for all points in a given angular distribution.

In order to compare more quantitatively the p-d and n-d angular distributions, it is useful to remove the effect of the Coulomb interaction from the p-d measurements so that the nuclear interactions themselves can be directly compared. Van Oers and Brockman[30] performed a phase-shift analysis of the nucleon-deuteron scattering up to about 40 MeV by varying the real parts of the phase shift up to $l=1$ and by varying the inelastic

TABLE VII. Born-approximation phase shifts.

Proton energy (MeV)	p-d without Coulomb force 36.0	p-d 36.0	p-d without Coulomb force 46.3	p-d 46.3
$^2\delta_2$	0.21 0153	0.24 6069	0.23 1805	0.27 4149
$^4\delta_2$	−0.05 5035	−0.06 4441	−0.03 1775	−0.03 7580
$^2\delta_3$	0.03 6521	0.04 2762	0.05 7394	0.06 7879
$^4\delta_3$	0.07 2748	0.08 5181	0.07 7033	0.09 1105
$^2\delta_4$	0.03 4008	0.03 9820	0.04 4506	0.05 2636
$^4\delta_4$	−0.01 0846	−0.01 2700	−0.00 5611	−0.00 6636
$^2\delta_5$	0.00 5106	0.00 5978	0.01 0969	0.01 2973
$^4\delta_5$	0.01 2543	0.01 4686	0.01 4674	0.01 7354
$^2\delta_6$	0.00 5835	0.00 6832	0.00 8754	0.01 0353
$^4\delta_6$	−0.00 2429	−0.00 2845	−0.00 1225	−0.00 1449
$^2\delta_7$	0.00 0913	0.00 1068	0.00 2401	0.00 2840
$^4\delta_7$	0.00 2732	0.00 3199	0.00 3317	0.00 3923
$^2\delta_8$	0.00 1641	0.00 1922	0.00 2401	0.00 2840
$^4\delta_8$	−0.00 0828	−0.00 0969	−0.00 0475	−0.00 0562
$^2\delta_9$	0.00 0565	0.00 0661	0.00 1056	0.00 1249
$^4\delta_9$	0.00 1344	0.00 1573	0.00 1479	0.00 1749
$^2\delta_{10}$	0.00 1304	0.00 1527	0.00 1587	0.00 1877
$^4\delta_{10}$	−0.00 0652	−0.00 0763	−0.00 0423	−0.00 0500

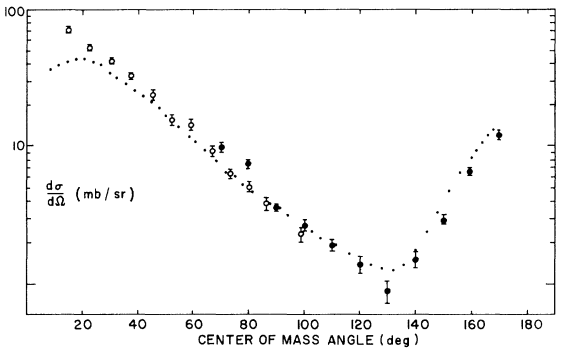

FIG. 7. Differential cross section for n-d scattering at 46.3 MeV. Open circles correspond to data taken with the liquid-scintillator-neutron-detector technique. Black circles are data taken with the solid-state-detector technique. The dots are UCLA measurements for p-d at 46.3 MeV.

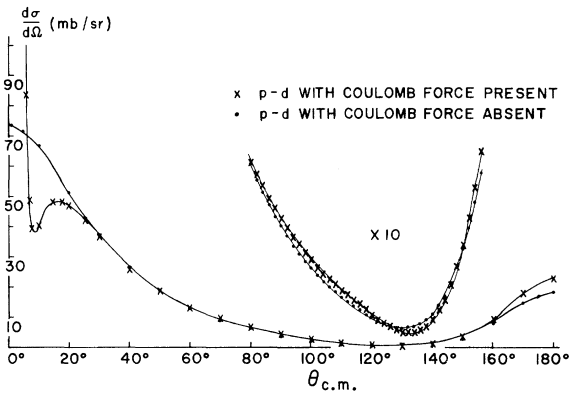

FIG. 8. Calculation of the effect of the Coulomb interaction in the elastic scattering of protons in deuterium for incident protons of 46.3 MeV.

parameters up to $l=2$. The analysis included a total of 11 partial waves. The real parts of the phase shifts with $2 \leq l \leq 11$ were calculated using the Born approximation and are not listed in that reference. The phase shifts for $2 \leq l \leq 10$ were calculated here independently in the Born approximation following Van Oers and Brockman's procedure.[30,31] The rest of the phase shifts are interpolated values obtained from Table II of Van Oers and Brockman.[30] Table VII lists the phase shifts used for 36.0 and 46.3 MeV.

Figure 8 compares the p-d differential cross section as observed with that which would be obtained with the Coulomb interaction absent as calculated by these phase shifts for the 46.3-MeV case. It is to be noted that removal of the Coulomb force raises the minimum in p-d scattering by a factor of 1.20. However, our experimental results indicate that the experimental n-d minimum is already deeper by about 30% than the p-d minimum observed experimentally. Thus removal of the Coulomb effect in this manner increases the difference between p-d and n-d scattering at the minimum. A similar situation occurs if one compares the n-d and p-d angular distributions at 36.0 and 35.0 MeV, respectively. The difference at small c.m. angles and at the minimum in the cross section appears to be significant and beyond the experimental error we can assign to our points.

A comparison of the experimental angular distribution for n-d scattering with dispersion calculations of the type N/D which includes tensor forces is in progress.[32]

The n-d differential cross section was integrated to give the n-d total elastic cross section. This was done by making a least-squares fitting of the differential cross section in terms of the Legendre polynomials. Table VIII presents the results for both energies by including seven and nine terms in the expansion. The goodness of fit is defined as

TABLE VIII. Least-squares fitting of the n-d differential cross section to the Legendre polynomial $\sigma(\theta_{\text{c.m.}}) = a_0 + a_1 P_1(\cos\theta_{\text{c.m.}}) + a_2 P_2(\cos\theta_{\text{c.m.}}) + \ldots$.

Legendre coefficient	36.0 MeV		46.3 MeV	
a_0	15.6	16.0	11.3	11.3
a_1	24.7	25.3	19.7	19.9
a_2	25.5	26.5	20.7	21.1
a_3	9.1	9.9	10.3	10.8
a_4	11.4	13.5	9.2	10.2
a_5	0.90	3.5	2.2	3.4
a_6	3.4	8.2	3.0	4.7
a_7		4.1		1.5
a_8		3.7		1.5
Number of parameters	7	9	7	9
Goodness of fit	4.40	3.30	3.94	3.7

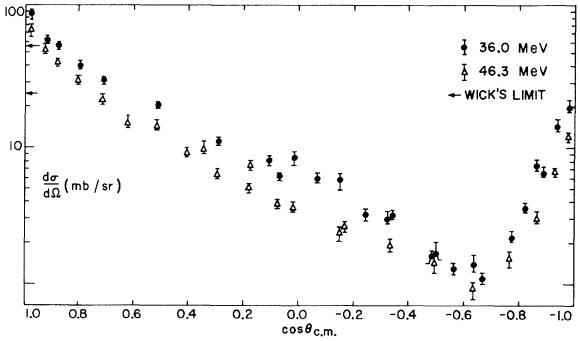

FIG. 9. The n-d differential cross sections plotted as a function of $\cos\theta_{\text{c.m.}}$. The arrows indicate the respective Wick's limits.

TABLE IX. n-d nonelastic cross section.

Energy (MeV)	σ_{total} (Ref. 28) (mb)	$\sigma_{el} = \int \frac{d\sigma}{d\Omega} d\Omega$ (mb)	$\sigma_{nonel} = \sigma_{total} - \sigma_{el}$ (mb)	σ_{nonel} (Ref. 30) (mb)
36.0	350 ± 3	196 ± 5	154 ± 6	140
46.3	262 ± 3	146 ± 3	116 ± 5	115

the total χ^2 divided by the difference between the total number of data points and the number of free parameters. From the constant term of this expansion we obtained the n-d total elastic cross section. Subtracting this from the measured n-d total cross section,[26] we obtained the n-d nonelastic cross section. Table IX shows these quantities. The last column shows the n-d reaction cross section estimated by Van Oers and Brockman[30] by using the p-d differential-cross-section data. No error is quoted but there appears to be reasonable agreement.

Figure 9 shows a plot of the logarithm of the differential cross section versus $\cos\theta_{c.m.}$ for the n-d data. The extrapolation to (+1.0, 0°) and (−1.0, 180°) is fairly direct. Also indicated in Fig. 9 is Wick's limit.[33] Our data are consistent with this lower limit.

We are indebted to Dr. J. Seagrave, Dr. R. Reid, and R. Walraven for helpful discussions and Dr. M. McGie for assistance in making the measurements. We would also like to acknowledge the ready assistance of the crew of the Davis 76-in. cyclotron. One of the authors (J.L.R.) acknowledges the support of the Convenio, University of California-University of Chile.

*Work supported in part by the U. S. Atomic Energy Commission under Contract No. AT(11-1) GEN-10, P.A. 15.

†Present address: Facultad de Ciencias, University of Chile, Casilla 653, Santiago, Chile.

‡Present address: Institute for Nuclear Study, University of Tokyo, Tokyo, Japan.

[1]L. D. Faddeev, Zh. Eksperim. i Teor. Fiz. 39, 1459 (1960) [transl.: Soviet Phys. – JETP 12, 1014 (1961)].

[2]A. M. Mitra, Nucl. Phys. 32, 529 (1962).

[3]R. D. Amado, Phys. Rev. 132, 485 (1963).

[4]R. Aaron, R. D. Amado, and Y. Y. Yam, Phys. Rev. 136, B650 (1964).

[5]A. C. Phillips, Phys. Rev. 142, 984 (1966).

[6]L. M. Delves and A. C. Phillips, Rev. Mod. Phys. 41, 437 (1969).

[7]L. A. Laroze and E. A. Harms, Bull. Am. Phys. Soc. 14, 493 (1969).

[8]I. H. Sloan, in *Proceedings of the International Conference on the Three-Body Problem in Nuclear and Particle Physics, University of Birmingham, 8–10 July 1969* (North-Holland Publishing Company, Amsterdam, The Netherlands, 1970), p. 34.

[9]J. D. Seagrave, unpublished.

[10]J. P. Burq, M. Chemarin, M. Gouanere, and G. Nicolai, in *Proceedings of the International Conference on the Three-Body Problem in Nuclear and Particle Physics, University of Birmingham, 8–10 July 1969* (North-Holland Publishing Company, Amsterdam, The Netherlands, 1970).

[11]J. Romero, J. A. Jungerman, Y. Ishizaki, and W. J. Knox, Bull. Am. Phys. Soc. 14, 553 (1969).

[12]J. P. Scanlon, G. H. Stafford, J. J. Thresher, and P. H. Bowen, Nucl. Phys. 41, 401 (1963).

[13]J. A. Jungerman and F. P. Brady, to be published.

[14]J. A. Jungerman, W. J. Knox, J. Romero, C. Badrinathan, F. P. Brady, T. A. Cahill, M. Kelly, and Y. Ishizaki, Bull. Am. Phys. Soc. 14, 4 (1969).

[15]C. J. Batty, B. E. Bonner, A. I. Kilvington, C. Tschalar, and L. E. Williams, Nucl. Instr. Methods 68, 273 (1969).

[16]B. M. Bardin and M. E. Rickey, Rev. Sci. Instr. 35, 902 (1964).

[17]R. Smythe, Rev. Sci. Instr. 35, 1197 (1964).

[18]J. C. Young, J. L. Romero, F. P. Brady, and J. R. Morales, Nucl. Instr. Methods 68, 333 (1969).

[19]F. P. Brady, J. A. Jungerman, J. C. Young, J. L. Romero, and P. J. Symonds, Nucl. Instr. Methods 59, 57 (1968).

[20]F. P. Brady *et al.*, Nucl. Instr. Methods 63, 358 (1968).

[21]Written by Dr. E. C. May.

[22]A. C. Berick, R. A. J. Riddle, and C. M. York, Phys. Rev. 174, 1105 (1969).

[23]B. E. Bonner, E. B. Paul, and G. C. Phillips, Nucl. Phys. A128, 183 (1969).

[24]R. Batchelor, W. B. Gilboy, J. B. Parker, and J. H. Towle, Nucl. Instr. Methods 13, 70 (1961).

[25]Written by R. Walraven.

[26]W. J. Knox, F. P. Brady, J. A. Jungerman, M. R. McGie, J. Romero, M. Auman, T. Montgomery, and R. Walraven, Bull. Am. Phys. Soc. 15, 475 (1970).

[27]F. P. Brady, W. J. Knox, J. A. Jungerman, M. R. McGie, and R. Walraven, to be published.

[28]F. P. Brady, W. J. Knox, J. A. Jungerman, M. R. McGie, and T. Montgomery, to be published.

[29]S. N. Bunker, J. M. Cameron, R. F. Carlson, J. R. Richardson, P. Tomas, W. T. H. Van Oers, and J. W. Verba, Nucl. Phys. A113, 461 (1968).

[30]W. T. H. Van Oers and K. W. Brockman, Jr., Nucl. Phys. A92, 561 (1967).

[31]R. S. Christian and J. L. Gammel. Phys. Rev. 91, 100 (1953).
[32]A. S. Rinat-Reiner, private communication.
[33] $\left(\frac{d\sigma}{d\Omega}\right)_W (0°) \leq \left(\frac{d\sigma}{d\Omega}\right)_{el} (0°)$,
where for n-d scattering
$$\left(\frac{d\sigma}{d\Omega}\right)_W (0°) = 30.28 \times \frac{E_{inc} m_n (\sigma_{tot})^2}{(1 + m_n/m_d)^2} .$$

PHYSICAL REVIEW C VOLUME 2, NUMBER 6 DECEMBER 1970

Proton-Neutron Final-State Interactions in the D(d, dp)n Reaction*

W. von Witsch, M. Ivanovich, D. Rendic,† J. Sandler, and G. C. Phillips
T. W. Bonner Nuclear Laboratories, Rice University, Houston, Texas 77001
(Received 10 April 1970)

The reaction D(d, dp)n has been studied at bombarding energies between 11 and 13 MeV. Two charged particles were detected in coincidence at pairs of angles corresponding to the recoil axes of the reaction D(d, d)d* where d* is a p-n system at zero relative energy. Time-of-flight and ΔE-E information were used for background subtraction and particle identification, respectively. The experimental spectra are dominated by strong peaks at low relative energies in the p-n system which are in part attributable to the isospin-forbidden formation of the "singlet deuteron." The shape of the experimental spectra is not predicted very well by either Watson-Migdal or Phillips, Griffy, Biedenharn theories.

INTRODUCTION

Complete three-body experiments have been used quite extensively in recent years as a means of studying nuclear resonances and final-state interactions. Of particular interest, of course, have been reactions which involve not more than three nucleons, since they allow the investigation of the $^1S_0$ nucleon-nucleon interaction with a minimum of interference from other final-state interactions. Several such experiments have been reported,[1-4] and the results obtained by various authors by fitting the data with the theories of Watson-Migdal (WM),[5] Phillips-Griffy-Biedenharn (PGB),[6] or with a modified Born approximation are encouraging although the experimental as well as the theoretical uncertainties are still very large. The next more complicated reactions, then, are those involving four nucleons, such as the D(d, dp)n reaction, which is the subject of this paper. This reaction has been studied by several authors[2,3] with regard to the quasifree scattering of deuterons from protons. The purpose of the experiment described here, however, was the investigation of the p-n final-state interaction in a reaction where the $^1S_0$ ($T = 1$) configuration is isospin forbidden. Although some evidence for the isospin-forbidden production of "singlet deuterons" in the reaction $^{12}C(d, pn)^{12}C$ has recently been reported,[7] no systematic study of this effect is known to us.

A kinematically complete experiment has been performed wherein protons and deuterons were detected in coincidence at angle pairs corresponding to the recoil axes in the D(d, d)d* reaction, where d* is a p-n system at zero relative energy. It was possible to observe final-state-interaction effects for relative energies in the p-n system between 0.0 and 2.0 MeV.

EXPERIMENTAL PROCEDURE

A deuteron beam, provided by the Rice University tandem accelerator, of about 50 nA was used to bombard a foil of deuterated polyethylene of about 300-μg/cm^2 average thickness. The elastically scattered deuterons were monitored at 30° in order to allow the extraction of absolute three-body cross sections,[4] using the d-d elastic scattering data by Wilson *et al.*[8] A ΔE-E detector telescope and a single E counter were used to identify p-d and d-p coincidences. The telescope was positioned at an angle of 30° in the laboratory, whereas the single counter was placed on the opposite side of the beam at angles of 44.5, 46.0, and 47.2° for bombarding energies of 11, 12, and 13 MeV, respectively. In this geometry, the p-d and d-p loci are kinematically well separated, but a considerable reduction of background resulted from the use of particle identification. The solid angles for both detectors were 1.04×10^{-3} sr. The beam was monitored in a Faraday cup in the conventional way.

Time-of-flight information was used to impose fast-coincidence requirements on the data, off